WIRELESS COMMUNICATIONS AND MOBILE COMPUTING
Wirel. Commun. Mob. Comput. 2012; **12**:53–70
Published online 8 January 2010 in Wiley Online Library (wileyonlinelibrary.com). DOI: 10.1002/wcm.889

SPECIAL ISSUE PAPER

A study on wireless sensor network based indoor positioning systems for context-aware applications

Jing Wang*, R. Venkatesha Prasad, Xueli An and Ignas G. M. M. Niemegeers

WMC/IRCTR, Delft University of Technology, Mekelweg 4, 2628CD Delft, the Netherlands

ABSTRACT

The newer context-aware applications require many inputs and amongst them the location information is one of the most important. In the near future, we see the potential in using wireless sensors deployed inside buildings to support in generating the location information besides their other routine tasks. This paper records the efforts involved in designing and prototyping a centralized indoor positioning system for tracking a target's position. We present an in-depth discussion on the RSSI based positioning algorithms both, range-based and range-free. Considering that the signal strength can be distorted heavily due to multi-path and shadowing, we have proposed the weighing schemes to leverage the credibility of the measured RSSI values. For online tracking, we have also proposed boundary selection and local grid scanning to lower the searching time, and the RSSI data dissemination and collection schemes to reduce traffic overhead. Evaluations have been done in both the field measurements and with an RSSI generator. The generator has been developed to simulate and replace the real measurements for the ease of algorithm design and testing, thus avoiding repetitive field measurements. The results show that positioning systems with adequate accuracy can be built with our proposed schemes. We expect that these proposed schemes to be integrated in multitude of systems with context-aware applications, which use location information

KEYWORDS

indoor positioning; RSSI; Tmote; context-awareness

***Correspondence**

Jing Wang, WMC/IRCTR, Delft University of Technology, Mekelweg 4, 2628CD Delft, the Netherlands.
E-mail: jing.wang@tudelft.nl

1. INTRODUCTION

With the emergence of new solutions for connectivity anywhere and everywhere [1] and with the concept of Ambient Intelligence [2,3] people have been expecting the imminent advent of a new network paradigm featured by context-awareness. The new paradigms securely connecting many heterogeneous nodes and/or networks have been proposed recently. European projects on wireless personal network (WPN) [4] and future home networks (FHN) [5], are both the examples where context-aware applications are thought to be an essential part of the applications in the mobility enabled networks. In a WPN the user and all the belonging devices are constantly and securely connected, and applications are adapted in such a way that the service sessions are transported seamlessly without the user's intervention depending on the context or situation. The context-aware solutions try to exploit information regarding geographical locations, time, available equipment and history of the user's interaction/usage, environmental changes, and the presence of other people [4]. Thus the services are provided in the way that most suited to the user's present situation. One of the important inputs for a context-aware application is the knowledge of the physical location of users and devices. Location awareness sustains important functionalities such as session transfer, self-organization and maintenance of the network. Since the location information is an important aspect of the context, it is necessary to implement the positioning system in a context-aware network efficiently. Thus we concentrate on localization, especially indoor positioning, in this paper. We have explored the promising positioning schemes to provide the location information with sufficient accuracy, i.e., room level for context-aware applications.

Global positioning system (GPS) [6] is currently the most successful positioning system available in the market. In the outdoor environment sufficient accuracy can be achieved with GPS. However, due to the distortion of satellite radio signals by various building materials and structures, GPS loses its effectiveness inside buildings, where a rich variety of context-aware applications are on demand. Alternatively, special sensing devices such as those with the infrared

beam and the ultrasound transmitter can be used for indoor localization. However, it would be better if many devices, already deployed, can be exploited for positioning along with their other usual tasks. With the rapid progress in the field of wireless sensor networks (WSN), sensors which are already deployed for specific tasks can be used in the meanwhile for generating the location information. An important resource used for finding location is the received signal strength, which can be easily acquired from the sensor network in the form of the Received Signal Strength Indicator (RSSI). In general, proposed RSSI-based positioning algorithms proposed can be classified as range-based and range-free. The range-based algorithms translate RSSI to the absolute location or distance by using the 'signature-based' implementation or triangulation method. However, many have pointed out that RSSI is vulnerable due to many factors, which largely degrades the performance of the range-based methods. On the other hand, the range-free algorithms exploit RSSI measurements by only comparing their values. This is expected to bring more error tolerance than the hard mapping done in their range-based counterparts.

Although the extensive localization techniques have been reported in the prior works, the prototyped position tracking systems we have studied mainly adopted simple algorithms. For example RADAR [7] and MoteTrack [8] used signature-based techniques, PetTracker [9] approximated the target's location as the closest anchor's location, and the enhanced RSSI-based tracking system in Reference [10] used simple triangulation method. Therefore, we believe it is of great importance to study positioning systems with the tailored localization algorithms, both range-based and range-free, for online tracking. To evaluate the feasibility of our proposed location algorithms under the real situations, we have prototyped an Online Person Tracking (OPT[†]) system, which can potentially be integrated into a larger framework of context-aware networks. A widely used wireless sensor device, Tmote-Sky [11] has been employed in our test-bed. Our system is simple and inexpensive containing a small number of sensor devices. Another contribution of this paper is that we have developed an RSSI generator to simulate the RSSI values by capturing statistical features of the field measurements. The generator eases the design and evaluation of algorithms by providing a more realistic RSSI input while eliminating many trivial settings and laborious measurements. This work discusses in great depth a detailed study of RSSI-based positioning system, implementations, lessons learned and the results thereof.

The rest of the paper is organized as follows: we first discuss some related earlier works on positioning techniques in Section 2; in Section 3 we present the calibration experiments for studying RSSI characteristics, based on which we propose three RSSI generator models; Section 4 introduces our algorithms, which are designed for prototyping our positioning system; Section 5 explains the simulation and test-bed setup and discusses the results of the simulation and the field experiments; and in the end we conclude our work in Section 6.

2. POSITIONING TECHNIQUES

2.1. Requirement for Indoor Positioning Systems

A reliable positioning system is critical especially for mobile computing environments. The positioning system must have the following features:

- *Adequately accurate*: the required accuracy always depends on the specific application. In the cases of WPNs and home networks, many context-aware applications like to know the place where the user is currently located. However, in most cases, if not very accurate, an approximate location of the user is required, so that as he/she moves it should be possible to find the next room he/she is going to.
- *Less complex*: as positioning systems mostly generate inputs for various advanced location-aware applications, it is required to be as lightweight as possible, which is in line with the concept of ambient intelligence—for responding in an unobtrusive and invisible way [2]. In most cases, it is unlikely that dedicated positioning devices will be deployed at high density and price. It is expected that positioning should be done as an additional function of the devices along with their routines, for example, access points and environmental sensors. Therefore, the system complexity is constrained by the power and computational capacity of the available devices. For online tracking real-time location information is required, thus computational complexity should as less as possible to get estimations timely updated.
- *Real-time*: one of the goals for context-aware application is to adapt itself to the new context where the user moves onto. The adaptation is based on the acquisition on the updated context. As the location information is among the most dynamic, it should be updated periodically at appropriate intervals. The update duration should be determined by the person's mobility and the building structure. Considering the moderate mobility with walking speed of 1 to 2 m/s as commonly seen in the indoor scenarios, the updating duration should be within a few seconds.

2.2. Earlier Studies on Positioning Systems

To acquire the location of a person, the most primitive way is to either ask the person to explicitly 'report' his/her location from time to time, or to infer the person's location *via*

[†] In fact the term OPT was used to symbolize 'Online Professor Tracking' since one of the professors was tracked during our first experimentation.

some of his/her traceable activities such as logging into the computer in different domains, etc. However, they are either disturbing (due to the requirement of active involvement by the person) or lacking in accuracy in case the person does not have any activity that can give these inferences. Thus they are hardly used. For this reason, many works have been done on the positioning systems which can automatically detect person's location.

Positioning systems adopt many approaches that are suited for different problems. Hightower and Borriello [12] developed the taxonomy to develop, evaluate and identify opportunities for location-sensing techniques in general. When we look into the approaches in detail, different positioning algorithms focus on different types of data explored [13]. The main techniques are based on Angle-of-Arrival (AoA), Time-of-Arrival (ToA), and the radio signal strength, which is mostly indicated by the RSSI.

Earlier studies that used AoA and ToA-based techniques have showed that a sufficient accuracy could be achieved in finding the range. Additional improvement can be obtained using Ultrasound and Ultra Wide Band (UWB) technologies with ToA measurements [14,15] or using AoA assisted ToA systems [16]. A survey on UWB-based localization can be found in Reference[17]. However, these systems require extra hardware support like antenna arrays, ultrasound and UWB transceivers to measure the time taken for the radio wave to propagate between the devices. Hence it increases the complexity of the devices and becomes expensive.

Studies on the radio propagation model have shown that given the transmitted signal power, the received signal strength is essentially related to the transmission distance. This motivates extensive researches on localization systems by making use of the radio signal strength.

GPS is one of the well-proven techniques. It is usually very effective for outdoor positioning. However, due to the dependency on expensive hardware as well as the inaccuracy and fallibility caused by the interference and multi-path fading inside buildings, GPS is not suitable for indoor positioning.

Alternatively, most signal strength based indoor positioning systems have been proposed to make use of the existing indoor networking facilities, such as WLAN system, RFID Tags [18] and especially, WSN. WSNs are gaining great popularity in the recent research and deployment, as more and more environment monitoring sensors have been deployed in many buildings in order to collect the data of the environmental parameters such as temperature, humidity etc. The environmental sensors along with the wearable sensors (e.g., used for monitoring one's health) can be exploited for finding the location of a person. This way it is more practical, cost effective and simple. In Reference [19], the authors provided an extensive survey of wireless senor network localization techniques. However, as pointed out in the same paper one of the challenging research topics is the problem of the noise distance measurement. For RSSI-based positioning techniques, the distance errors are mainly due to the unreliable RSSI measurement. Ideally RSSI value monotonically decreases with the increase of distance according to the Log-distance path loss model. However, RSSI value is easily affected by the imperfect omni-directional antenna pattern, as well as by the indoor conditions such as obstructions and human activities that cause multi-path fading and shadowing. This can violate the monotonically decreasing relation; for example, at the fixed distance between the transmitter and the receiver, multiple RSSI values can be measured if the transceiver pair is placed at different places. The distance estimation from RSSI measurement is greatly challenged by the lack of a universally applicable indoor propagation model that could be employed in different types of building structures and antenna patterns. Further, a unified model is also difficult to achieve. Thus the earlier investigations have mostly focused on the estimation algorithms to minimize the effect of the unreliable RSSI measurements.

RSSI-based positioning algorithms can generally be divided into two categories: *Range-based* and *Range-free*.

Range-based algorithms use the absolute distance or angle calibrated from the pre-measured RSSI map, which can be in the form of 'signatures' or a RSSI to distance/angle relation map. Radio signatures are collected at various indoor locations at the off-line stage, and are stored in the database with the corresponding locations. During the online positioning, the system matches the RSSI acquired by the mobile target and the signatures in the database to map the target with the known locations. Prototype examples for such systems are RADAR [7] and MoteTrack [8], which can achieve accuracy with a mean error distance of 2–3 m. Further in Reference [20], the coefficients of Fourier transformation of the RSSI (RSS-DFT) were used as the signature, which improved the positioning with the average error of about 1.5 m. Instead of constructing a database of signatures, target's location can be estimated by triangulation using the RSSI-distance relation mapping. That is, given the RSSI values of the reference points (called anchors now on), which are aware of their own positions, the distance between the target and the anchors can be found from a pre-calibrated relation map. With three (or more) distances, the location of the target can be fixed. A commonly applied method is the Minimum Mean Square Error (MMSE) estimation, examples as: the enhanced RSSI-based tracking system in Reference [10], AHLoS in Reference [14] and the autonomous localization method in Reference [21].

Instead of using the RSSI to map the absolute locations, range-free algorithms utilize the geographic relationship between targets and anchors. We can further group range-free techniques as *the geographical constraint* and *the hop constraint*. The geographical constraint techniques explore the location information of anchors within the range of the target. One of the simplest methods as used in the PetTracker system [9] is to compare the target beacon packets' RSSI of the neighboring anchors and approximate the target's location by picking the location of the anchor that receives the highest RSSI. In Reference [22] the authors proposed a Weight Centroid Localization (WCL) algorithm, which weighed the known locations of the anchors in the range by

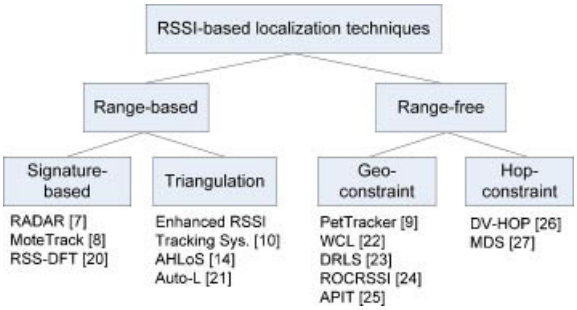

Figure 1. Overview of RSSI-based localization techniques, with the examples referred.

exploring the RSSI. The weights were calculated relying on the extensive pre-measurement of the RSSI values at two different frequencies and 15 different transmission power levels. A similar approach was proposed in Reference [23], where a grid-scan was used for initially finding the target's position and further this position was refined with the information of the non-neighboring nodes. Whereas in the methods of [9,22,23] each geographical constraint is made from the single neighbor anchor, in the proposed Ring Overlapping based on Comparison of RSSI (ROCRSSI) method [24], each ring shaped constraint area was generated by using the RSSI relations between the target and two neighbor anchors. A series of overlapping ring shape constraint areas were used to narrow down the possible area in which the target resides. Similarly the Approximate Point In Triangulation (APIT) method [25] explored every time three neighbor anchors to generate one triangular constraint area. The hop constraint techniques estimate target's location by using the hop count information from certain anchors that is not necessary the one-hop neighbor of the target. Examples are DV-HOP [26] and MDS [27]. The hop-constraint techniques are mainly designed for large scale sensor networks and combining with certain routing algorithms.

An overview of the RSSI-based algorithms is presented in Figure 1. Comparatively, range-free algorithms release the laborious off-line measurements, and are supposed to have large margin to tolerate the RSSI error since the RSSI values are used only for comparison; while range-based algorithms are generally simpler in terms of the algorithm structure.

3. RSSI GENERATOR

RSSI measurement usually involves many trivial settings and laborious work. Keeping the goal of the field measurement, which is to evaluate the performance of the positioning algorithms under the realistic situations, it can be useful to design an RSSI generator to replace the real measurement for the ease of the algorithm design. The RSSI values generator should be able to generate the RSSI at a given distance with the characteristics expected from the field measurements. By using the RSSI generator one can study all the algorithms and compare them without going through the laborious process of implementing them on test-bed while keeping the environmental characteristics constant for a better comparison. It is very difficult to get the similar conditions for RSSI-based measurements in practice, thus no two measurement sets are same. The advantages of using RSSI generator are, (a) less time required for evaluating and validating algorithms and, (b) a stable framework for comparing many algorithms with the identical RSSI set.

3.1. RSSI Characterization

Before going into the RSSI generator details, we first explain the calibration experiments which shed the light on the characteristics of RSSI.

3.1.1. Tmotes.

In the calibration experiments, we have employed the widely used sensor hardware—*Tmote Sky*, which are based on Telos Revision B platform [11]. Tmote features the Chipcon CC2420 radio [28] for wireless communications. The CC2420 has an IEEE 802.15.4 compliant radio. The network stack is implemented in TinyOS [29] which is an event-driven operating system designed for the sensor platforms with limited computational and memory resources. The sensor platform has been developed using NesC [30]—an extension to the C programming language designed to be used with TinyOS.

3.1.2. Antenna pattern.

The first experiment has been designed to see the dependence of the RSSI value on the antenna orientation. Tmote's internal antenna is an inverted-F micro-strip that does not have a perfect omni-directional pattern. We have conducted a simple experiment to know how the antenna orientation affects the RSSI values. We placed two motes with fully charged batteries acting as the transmitter and the receiver 4 m apart in the line-of-sight, and measured the RSSI values at 8 different relative antenna directions from 0° to 360° in steps of 45°. During the measurements each Tmote was placed on top of a Styrofoam cube (width: 5 cm, depth: 5 cm, height: 15 cm) on the linoleum floor. For each direction, we collected the RSSI values in 5 minutes, at a rate of 4 packets per second, that is, 1200 samples have been taken. Figure 2 shows that the antenna has the strongest signal strength at 0° about -50 dBm, and the smallest signal strength at 90° about -65 dBm. Thus the RSSI value varies in a range of around 15 dBm.

3.1.3. RSSI *versus* distance.

For generating the empirical relationship on RSSI *versus* distance, RSSI has been collected by placing two Tmotes in the middle of a narrow corridor (60×2 m) at various

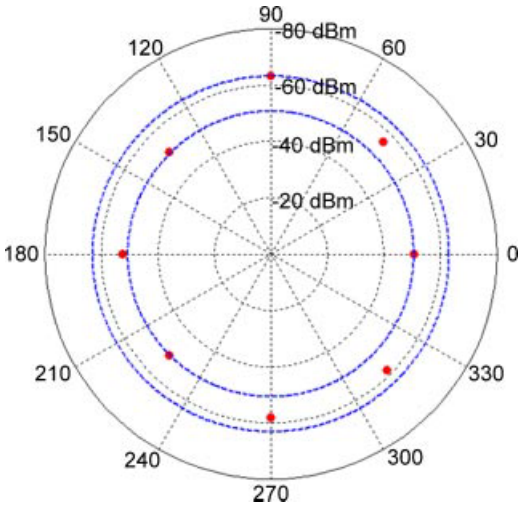

Figure 2. Antenna orientation measurement.

distances in between. According to the specifications Tmote's radio range is up to 50 m. However, it has been found that after 16 m, the packet drop percentage increases considerably [31]. Therefore, we would like to operate Tmotes within this range. As also observed in the previous work [25], the variations in measured RSSI is higher when the Tmotes are closer to each other—in order to get a better resolution at short distances—we took measurements from 0 to 1 m with a 0.2 m step, and from 2 to 16 m with 2 m step. For each distance, RSSI was measured with the receiver antenna direction of (0°, 90°, 180°, 270°) with respect to that of the transmitter. Other setups have been kept the same as described in Subsection 3.1.2. As shown in Figure 3, the measured RSSI values vary at each given distance, and in the worst case up to 30 dBm.

3.1.4. RSSI characteristics.

From the calibration experiments we can point out the following facts on RSSI characteristics based on our setups:

- RSSI value decreases with the distance in general.
- RSSI value also varies at the fixed distance. This is firstly due to the antenna orientations of the transmitter and the receiver; and secondly, due to the indoor environment, such as floors, walls, furniture, and people around etc., which cause multi-path fading and shadowing and thus ravage the monotonically decreasing trend of RSSI with the increase in distance.

3.2. RSSI Generator

Taking into account the statistical characteristics of RSSI at every distance, we have designed three models for the generator—1) the one based on the empirical probability mass function (pmf) of the RSSI measurement; 3) the statistical distribution best fitting the empirical pmf; and 3) the simplified model with a uniform distribution bounded by the collected RSSI values.

3.2.1. Generator–real model.

In this model, the empirical pmf of the RSSI measurements at a given distance has been calculated, as shown in Figure 4 the example of the distance at 4 m. The simulated RSSI is generated exactly according to the probability at each possible RSSI value, which has been obtained in the field measurement.

3.2.2. Generator–statistical model.

In this effort, we fit the empirical pmf into one of the probability distribution functions. By doing so, we expect to gain a general statistical model to minimize the errors due to the difficulty in carrying out the exhaustive measurement having samples on any distance with any antenna orientation. As the variation of RSSI values at a certain distance can be assumed being small, independent effects (e.g., multipath fading and shadowing) additively contributing to each measurement, we have considered

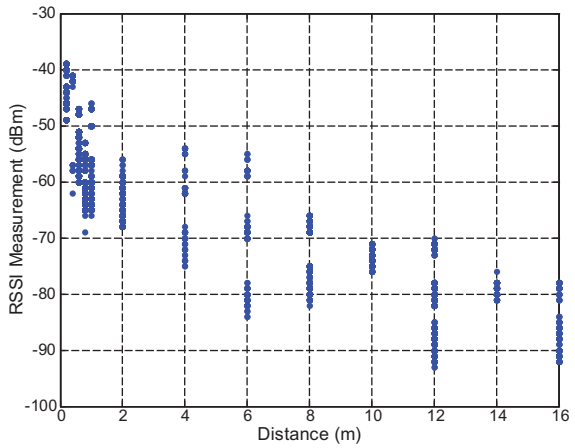

Figure 3. RSSI *versus* distance measurement.

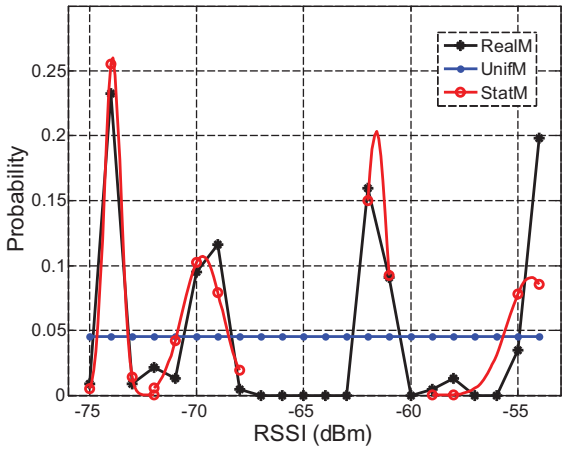

Figure 4. Generator models.

normal distribution as the one to start with. An observation from the empirical pmf is that the most of the measured RSSI values are close to one of the several values (the peaks, in Figure 4), due to the measurement being made in four different relative antenna directions between the transmitter and the receiver. In this case, if we want to minimize this variation, it is more appropriate for us to fit the statistical model according to the empirical pmf at individual antenna directions.

To test the normal fit, at each antenna direction we first check the fitting with χ^2 *goodness of fit* test. If the test result shows positive, a normal distribution is considered to represent the statistical characteristic of the observed RSSI measurement; if not, we take several other types of the distribution as the hypothesis. We have considered Poisson, Exponential and Normal distributions as the candidates, but it is easy to include more types of distributions. The hypothesized distributions are evaluated by comparing the root mean squared error (RMSE), which has the form:

$$\mathrm{RMSE} = \sqrt{\mathrm{E}\left(\left(\mathrm{RSSI}_{\mathrm{generated}} - \mathrm{RSSI}_{\mathrm{measured}}\right)^2\right)}$$

3.2.3. Generator–simplified model.

In this simplified model, we have considered a random number generator with uniform distribution. The motivation behind this is to test the usability of a very simple generator model to simulate the field measurement of RSSI, at the same time providing certain flexibility. The lower and the upper bounds are calculated by fitting the empirical RSSI values at a given distance into a uniform distribution with a confidence level of $(1-\alpha)\%$. To increase the flexibility of the generator, we added another parameter β_E to extend the bounds to β_E percentage of the original values. That is, the larger the β_E we take, the generated RSSI values are expected to be more different than the measurement values.

4. ALGORITHMS IN PROTOTYPE

As we investigate localization systems for providing location information for context-aware applications, particularly in the indoor environments (e.g., home networks and office networks), it is reasonable to consider the existence of context server(s) in the network to make the context information available for multiple applications. Meanwhile the indoor networks are typically of small or medium size, and thus do not suffer severe scalability problem. Therefore, we consider here a centralized localization system, which has additional advantages making it able to (i) access more comprehensive measured data from the network; (ii) use more sophisticated estimation algorithms as normally the central processing unit is a computer with sufficient storage, power and computational resources; and (iii) reduce the energy consumption burden on the sensor nodes as the major computation is done at the central processing unit. The disadvantage of the centralized system is the additional traffic imposed on the network as the measurement data need to be sent from individual sensor nodes to the central processing unit for further actions. Therefore, special considerations should be made during the design phase.

Since using the centralized systems relaxes the constraint on the complexity of estimation algorithms, we primarily investigate those algorithms focusing on estimation accuracy. To get more insight on both range-based and range-free algorithms for indoor location estimations, we have started from the conventional MMSE [14] and the concept of ROCRSSI [24] as the representatives, respectively. Considering that in the indoor environment the signal strength can be distorted heavily by multi-path fading and shadowing effects, we have proposed the weighing schemes for both algorithms to leverage the credibility of the measured RSSI values. Besides, under the special concerns on supporting the quickly updatable online tracking application, we have proposed the boundary selection and local grid scanning to lower the searching time for both the algorithms, the RSSI dissemination scheme for the sensors to reduce the traffic overhead in the network and the RSSI collection scheme for the central processing unit to update estimation in a timely manner. The following sections explain in detail on the proposed algorithms.

4.1. Range-based Algorithms

Three range-based algorithms have been developed in our prototype as comparison, and further we select the one that offers the least error for the online tracking implementation.

4.1.1. Algorithm 1: conventional MMSE (C-MMSE).

Minimum Mean Square Error (MMSE) has been a popular positioning technique, which is employed for the target location estimation using the distance *versus* RSSI relation map. We reproduce the MMSE algorithm here for the sake of completeness. We let the moving target send beacon packets, and the anchors collect the instantaneous RSSI values of the beacons. The locations of the anchors are known *a priori*. As illustrated in Figure 5(a), let us assume that N anchors are used for monitoring, and d_i is the estimated distance between the target Tmote, T, and an anchor, $i(\forall i, i = 1, 2, 3, \ldots, N)$which is located at (x_i, y_i),

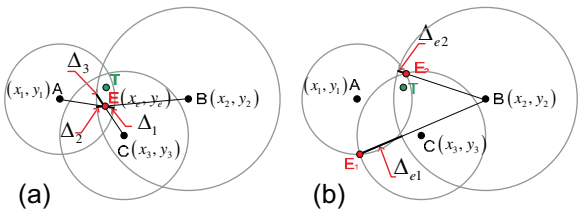

Figure 5. Illustrations for algorithms C-MMSE and M-MMSE. (a) Conventional MMSE. (b) Modified MMSE.

using the pre-calibrated RSSI *versus* distance relation. Error in estimation is defined as

$$\Delta = \left(\sum_{i=1}^{N} \Delta_i^2 \right)^{\frac{1}{2}} \tag{1}$$

where

$$\Delta_i = f_i(x_e, y_e) = \left| d_i - \sqrt{(x_i - x_e)^2 + (y_i - y_e)^2} \right| \tag{2}$$

and (x_e, y_e) is the estimated position in two-dimensional coordinates, which is sufficient in most of our cases. The estimated position (x_e, y_e) is obtained by minimizing Δ over a cross-sectional region, which depends on the error bounds on the distances using empirical RSSI *versus* distance relation. Based on the measurement shown in Figure 3, we averaged RSSI over the four antenna orientations, and drew the empirical relation (curve). As shown in Figure 6, the averaged RSSI decreases with the increase in distance between the sender and the receiver, but the rate at which RSSI decreases is different at different distance. For example, RSSI drops more rapidly within the range from 0 to 4 m. That is, the RSSI is more sensitive to the distance variation comparing to the cases where distance between two Tmotes is larger than 4 m. The sensitive RSSI is helpful to provide high resolution estimation, but it is also vulnerable to the environmental influence, as a small RSSI error may lead to serious displacement.

This most primitive MMSE method is referred here as C-MMSE method. The complexity of C-MMSE is much dependent on the number of anchors involved in estimating (x_e, y_e). For the RSSI-based estimation method with more number of anchors resulting in more d_i-s does not guarantee a higher accuracy. In many instances, this may result in a bigger error range. RSSI averaging over many neighbors does not yield better performance as tested in Reference [7]. Thus in our prototype we have chosen to use only three anchors with the strongest RSSI values for the algorithms presented in later sections.

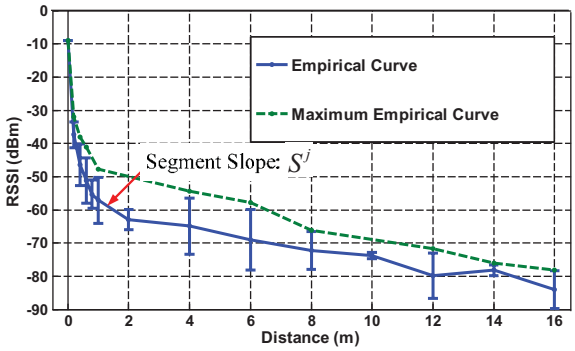

Figure 6. Experimental measurements: RSSI *versus* distance.

4.1.2. Algorithm 2: modified MMSE (M-MMSE).

M-MMSE simplifies C-MMSE by adopting the 'qualitative weighing' concept. Consider the situation where two anchors are nearer the target and the third one is farther away. Since estimated distance from the farther anchor generally has less accuracy than that of the closer anchors [31], thus amongst the three RSSI values, we assume that the first two highest RSSI values offer higher reliability than the third one. Therefore, in M-MMSE, only two anchors with the highest RSSI values are involved in the MMSE estimation process. This results in two possible positions. The third anchor is used to make the final decision among the two candidate positions. As shown in Figure 5(b), E_1 and E_2 are the candidate target positions estimated by anchor A and C. Δ_{e_1} and Δ_{e_2} are the estimated differences according to anchor B's RSSI value. The final estimation is chosen from E_1 and E_2, which has $\min(\Delta_{e_1}, \Delta_{e_2})$. The advantage of this method is that we have less searching area while looking for MMSE estimation, and thus it is faster. Moreover, since the third RSSI value is likely to have less accuracy, we use it qualitatively to avoid a larger error range in the estimation.

4.1.3. Algorithm 3: weighted MMSE (W-MMSE).

In M-MMSE the lowest RSSI value (having the lowest reliability) out of the three is only used to make the final choice from the two possible locations. We extend the same idea—that the reliability of the estimated distance is low if the anchor is far away from the target—to all the RSSI measurements from the anchors. Before calculating the target position by MMSE, we have processed all the measured RSSI values, and thus the corresponding distances, with different weights, which depend on the reliability of the measurements. A quantitative analysis of the reliability that is reflected in finding the weights used in this algorithm is discussed below.

Actually there is no explicit way to give a clear picture about the reliability with respect to the measured RSSI. Therefore it may be more applicable to consider that the fidelity of the converted distance is higher if the corresponding RSSI value is higher. Thus we have investigated the accuracy of the position measurements by giving higher priority to those with larger RSSI values. Intuitively, we have turned back to the experimental measurement of RSSI *versus* distance relation shown in Figure 6. To calculate weights, we have considered using the slopes, which are the piecewise linear approximation of RSSI *versus* distance curve resulting in segments. This is sensible as generally the steepness of the slopes in the empirical relation reflecting the RSSI value, thus the reliability of the RSSI measurement.

We have quantified the weights with the slopes of the line segments of the empirical curve. We have found various slopes in the empirical relation as shown in Figure 6, and then we have used them to modify the distances estimated

from the empirical relation with different weights. For each RSSI value we can find a slope S^j from the empirical relation for the jth segment of all P segments on the curve. If we have N anchors, out of them we select a set of three anchors that have the highest RSSI values. Let us call this set of three anchors as $M = \{k, l, m\}$. First, we find the distance $d_i, \forall i, i \in M$ from the empirical relation. S_i^j is the absolute slope found from the empirical curve for the anchor i with an RSSI corresponding to the segment j in the empirical relation, as shown in Figure 6. Then we define $\overline{w_i}$ to be the weight for anchors i, as:

$$\overline{w_i} = \frac{S_i^j}{\max\{S_i^j\}}, \quad \forall \{i, j\}, i \in M, j \in P \tag{3}$$

The W-MMSE is constructed as

$$\Delta_{\text{new}} = \left(\sum_{i=1}^{N} \overline{w_i} \cdot \Delta_i^2 \right)^{\frac{1}{2}} \tag{4}$$

and estimated position (x_e, y_e) is obtained by minimizing Δ_{new}.

4.2. Range-free Algorithm

The range-free algorithms eliminate the requirement of the absolute point-to-point distance estimation. Taking [24] as an example, the main idea is that each anchor generates a series of overlapping rings based on the comparison of RSSI to confine the possible area in which the target resides.

If the target as well as all the anchors in the network broadcasts beacon packets, the anchors can receive beacons from both the target and the other anchors. As RSSI value is related to the transmission distance, by comparing the RSSI of the beacons from the target and the other anchors, it is able to find an area, which is bounded by the anchors, and the target is likely to be inside. As illustrated in Figure 7, anchor A receives the RSSI values from anchor B, anchor C and the target T. The RSSI values have the relationship as $\text{RSSI}_{\text{AB}} > \text{RSSI}_{\text{AT}} > \text{RSSI}_{\text{AC}}$, therefore the target T is expected to lie in the grey ring. Similarly rings centered at other anchors, e.g., anchor B, can be generated. With a series of rings centered on the anchors, the estimated position is taken as the center of gravity of the final intersectional area of these rings. We refer to Reference [24] for the details. The non-isotropic path loss is considered in Reference [24] and a grid-scan algorithm is employed in Reference [25] to reduce the influence of the unreliable rings. However, in practice, RSSI is not only influenced by non-homogenous radio propagation, but also it is severely affected by the antenna pattern and building structure. Therefore the algorithm is very likely to suffer with the inaccurate information. For example, if the RSSI values received by anchor A have the relations, $\text{RSSI}_{\text{AB}} < \text{RSSI}_{\text{AT}}$ and $\text{RSSI}_{\text{AT}} < \text{RSSI}_{\text{AC}}$, no ring can be generated. Therefore we have proposed a range-free algorithm, which is designed to solve such problem by utilizing additional functions such as reliability testing, weighing and the flexible centering schemes.

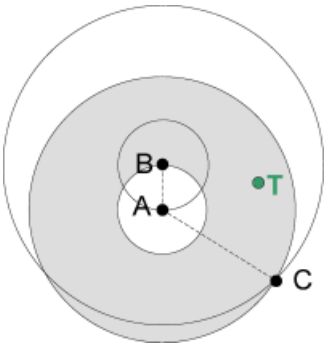

Figure 7. An illustration on ranging the target location by comparing RSSI values.

4.2.1. Reliability testing.

To solve the unreliable RSSI measurements problem discussed in the previous section, we have proposed to use a reliability test in our range-free algorithm. Motivated by the same reason as that in W-MMSE, we consider lower reliability if the RSSI value corresponds to a longer distance, and thus is likely to have a bigger estimation error.

In the design of the algorithm, each anchor has a neighbor list (ND) sorted in descending order based on the received RSSI values. For example, in Table I, anchor 6 decides that target T (Node ID 1) is in the ring between anchor 5 and anchor 7. However, if $d_{65} > d_{67}$, the ring cannot be generated. Therefore, we refer to target T's ND. T also has a sorted ND based on the received RSSI from the anchors, as shown in Table I. In T's ND, the RSSI from anchor 5 is higher than the RSSI from anchor 7, which suggests that RSSI from anchor 5 have higher reliability than the RSSI from anchor 7. Therefore, we ignore anchor 7 and move to anchor 3. If anchors 5 and 3 can generate a ring, we proceed to the next step. If anchors 5 and 3 still cannot generate a ring, we go back to trust anchor 7 and ignore anchor 5. If anchor 2 and 7 can generate a ring, then algorithm proceeds further. The accuracy of the reliability testing process is based on the assumption that the majority of RSSI values

Table I. Example neighbor list.

Target ND (ID1)		Anchor ND (ID6)	
Anchor ID	RSSI (dBm)	Node ID	RSSI (dBm)
2	−54.387	4	−64.7273
3	−83.801	8	−66.3333
4	−73.778	2	−76.4667
5	−65.529	5	−78.5714
6	−80.029	1	−80.0294
7	−82.002	7	−82.7143
8	−85.791	3	−88.6316

are reliable. Although RSSI can be disturbed by multiple factors, the above assumption is usually true in most of the situations.

4.2.2. Weighted overlapping.

Grid scanning algorithm has been employed to calculate the center of gravity of the intersection area. In Reference [24,25], the entire area was divided into small grids, and each grid maintained a counter, which was initialized to 0. If a grid was covered by a ring, the grid counter was increased by 1. After all the rings were generated, the intersection area was selected as the coverage of the grids with the highest count. The estimated position was found as the center of gravity of the intersection area. However, there are two aspects lacking of justification: (i) during the estimation process, as the counter is increased by 1 if the gird is covered by a ring, thus the unreliable rings have the same contribution as the rings with higher reliability; (ii) the estimation considers only the intersection area with the highest counter value, which in worst situation can be largely contributed by the unreliable rings. Taking Figure 8 for example, a wrong selection of the intersection area is made because of the influence of the unreliable ring.

Therefore we have proposed the *weighted overlapping*. Similar to assigning weights to the distances mapped by RSSI in W-MMSE, weighted overlapping means that different rings are assigned with different reliability weights to influence the estimation. When covered by a ring, the grid increases its counter scaled by the reliability weight of the ring. For the ring with center at anchor I, the reliability weight is defined as

$$w_{\mathrm{TI}} = \left(\frac{1}{\mathrm{RSSI}_{\mathrm{TI}}}\right)^{n} \tag{5}$$

where

- $RSSI_{\mathrm{TI}}$ is the RSSI value received from anchor I by target T.
- n is the power index related to the exponential index of the radio propagation model. More details on setting n are given when we discuss the experimental results in Subsection 5.2.5.

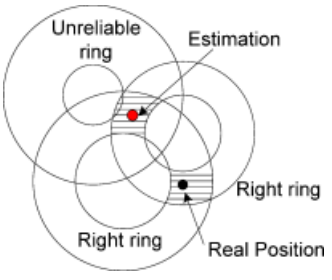

Figure 8. Influence of the unreliable ring.

4.2.3. Center of gravity selection of the intersection area.

In order to investigate the center of gravity selection based on the grid counter, different scenarios have been considered. After generating series of rings, three biggest grid counter values are selected and noted by $\{\max_i\}_{i=1,2,3}$, which satisfy ($\max_1 > \max_2 > \max_3$). Respectively, we have defined the 'max-i' scheme, in which the girds with the counter values not smaller than $\max_i$ are selected as the intersection area. The target position is estimated as the gravity center of the chosen intersection area.

4.3. Considerations for Fast Updating

For the online tracking system, the positioning update should be fast enough in order to give the real-time estimation. Two factors can affect the update speed. One is the time taken by the algorithm for computation; the other is the frequency of the estimation updates, more specifically, the time needed by the system to collect enough raw data for the next estimation. To reduce the algorithm computational complexity we have employed the boundary selection scheme to narrow down the range of the exhaustive searching in range-based algorithms, and in range-free algorithm we have used the local grid method to reduce time and memory consumption. To collect as many useful data as possible during the limited time interval, we have proposed an efficient data dissemination and collection scheme.

4.3.1. Boundary selection for range-based algorithms.

As described above, range-based algorithms use intersecting circles to determine the possible cross-sectional area, and then apply the exhaustive searching in the area yielding the optimal location estimation on the resolution that is sought. However, the exhaustive searching in a large area with fine resolution is computational and time consuming. In order to reduce the complexity and at the same time to maintain sufficient accuracy, bounding the searching area is necessary. The wider the area is bounded, it is more likely to cover target's position, but consumes more time since the system needs to search over a larger area. However, if the bounded searching area is too small, computations can be reduced but there is a chance of excluding the target's position from the searching area.

Because of the antenna orientation effect [32], the empirical relation between distance and RSSI has been found by averaging the RSSI values sampled from four different directions. Nonetheless, the mapped distance found from empirical relation for circular overlapping may induce potential error because of the exclusion of the real orientation. As shown in Figure 9, in order to include all the possible locations and at the same time to keep the computation cost as low as possible we define a maximum empirical relation as shown in Figure 6, which is constructed by using the maximum RSSI values of the measurements on

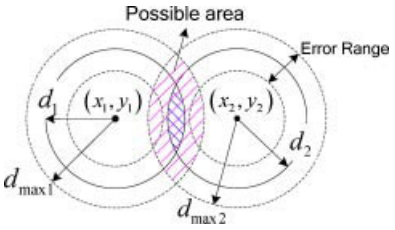

Figure 9. Estimated area selection.

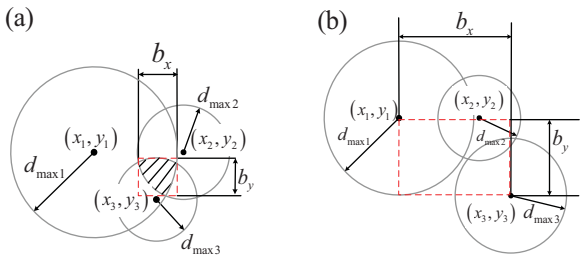

Figure 10. Boundary selection for range-based algorithms. (a) With overlapping area. (b) Without overlapping area.

four antenna directions at each distance, and further filtering out the points that violate the monotonically decreasing trend. In this way, we can find the maximal possible distance corresponding to certain RSSI to reduce the chance of missing target's location.

Consider using three anchors with their estimated distances to generate three circles. If the three circles are partly overlapping as shown in Figure 10(a), the target has higher possibility of being in the overlapping area. The searching range for $b_x$on x-axis varies from $\max\{x_1 - d_{\max 1}, x_2 - d_{\max 2}, x_3 - d_{\max 3}\}$ to $\min\{x_1 + d_{\max 1}, x_2 + d_{\max 2}, x_3 + d_{\max 3}\}$, where, $d_{\max i}$ is the distance found from the maximum empirical curve. If the three circles do not have a common overlapping area, as shown in Figure 10(b), then we let b_x to be ranging from $\min\{x_1, x_2, x_3\}$ to $\max\{x_1, x_2, x_3\}$. In this case without the common overlapping area, we expand the estimation area to increase the change that the potential target location is included in the search area. The same procedure is applied to find b_y. Another consideration is the building structure, as the selected boundary cannot exceed the physical dimension of the building, which sets limit on the search area.

4.3.2. Local grid scanning for range-free algorithm.

As previously proposed in Reference [24,25], the grid scanning method have been employed to calculate the center of gravity of the intersection area. In those works, the whole testing area was divided into small grids, each of which manipulates a counter. An important point missed there was the scalability of the system. As the tracking area can include large space or extend to several floors, it will be extremely resource inefficient if we also store the grids for the area far away from the target. Therefore, we have considered a local grid method for using the range-free algorithm for our tracking system. Rather than forming the grids for the entire building plan and storing all of them in the memory, we only record the grids that are useful for locating the target, that is, only the area confined by the rings or circles generated by the first n anchors are divided into grids. The first n anchors refer to the anchors that receive n biggest RSSI values from the target's beacons among all the deployed anchors. In our experiment, n takes 3. An illustration is shown in Figure 11, where the grid area is bounded by the rings of the anchor B, C and D, the three anchors nearest to the target. And the rings of A and E only partially affected the grid counters for the parts of the rings lying within this grid area.

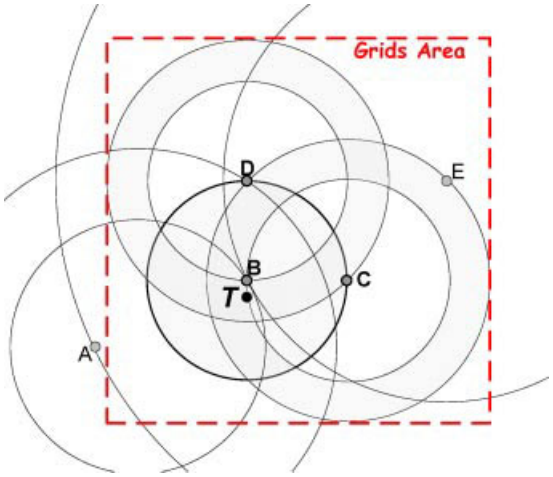

Figure 11. Local grids area selection.

4.3.3. Data collection.

In our tracking system, the target (for both range-based and range-free cases) broadcasts beacon packets periodically. Especially for the range-based case, no anchor but only the target sends beacons to reduce the total number of beacons needed and to avoid signal strength being affected by the anchors with different battery volumes. When an anchor receives the beacon packet, it measures the RSSI value, and unicasts the measurement to the computer, on which the position estimation algorithm runs. To meet the real-time requirement as discussed in Subsection 2.1, time for data collection needs to be minimized. However, acquiring enough data is inherently required by the positioning algorithms to use RSSI by smoothing out the irregular values. According to our experience, 60 RSSI values should be sufficient for each estimation. Shortening the data collection time can be achieved by making beacon packets sent out with higher frequency. However, as the sensor devices use the contention-based MAC protocol, it will increase the chance of packets collision, and may result in high back-off time at each anchor, especially when a large number of anchors are deployed within the radio range.

Alternatively, we make each anchor buffer several RSSI data and pack them into one packet instead of immediately sending out the RSSI data just received. In this way, the total number of the packets is reduced. At meanwhile, as several RSSI data share the same packet header, the total number of bits sent out by the anchors is also reduced, which is particularly appreciated for the power constrained sensor network.

5. TEST-BED SETUP, RESULTS AND DISCUSSIONS

5.1. Test-bed Setup

5.1.1. Test-bed environment.

The test-bed has been built on the 19th floor of our faculty building. The main part of the floor being used consists of eleven office rooms and one (large) student room. The dimension of an office room is 5×4 m, the student room is 5×12 m. The corridor in the middle is 2 m wide.

We have conducted the experiments during the normal working hours, when human activities have been involved such as people moving around, opening and closing the doors randomly. The target Tmote has been worn by a person. In the experiments the person may move in the corridor or change his stay among those twelve rooms. We have compared the positioning accuracy under different range-based algorithms and between range-based and range-free algorithms. For deploying the anchor Tmotes, we have considered two different patterns—triangular and rectangular patterns with various distances (2, 4, and 8 m) between the anchor Tmotes to evaluate the range-based algorithms. For the range-free algorithm, the deployment of the anchor Tmotes has been adopted a more random pattern. The deployment patterns have been designed for shedding light on the performance of the algorithms designed for the positioning system. The deployment has been tested independently for both range-based and range-free cases with respect to various combinations to achieve the best possible accuracy. We refer the results of the experiments in Reference[33] for brevity. Based on the estimation accuracy under different deployments, the ones with the best performance are further implemented for the real-time location estimation. For the range-based case, all the anchor Tmotes have been deployed in the corridor, with the horizontal distance between any two closest anchors being 4 m, as shown in Figure 12(a). For the range-free case, the anchor Tmotes have been deployed in the rooms, as illustrated in Figure 12(b).

5.1.2. Graphic user interface.

In order to visualize the real-time positioning of the target Tmote, we have developed an application with graphic user interface (GUI) to depict the floor plan of the building in Java programming language. It displays the person being tracked with a red dot, which is updated after each estimation. Some GUI snapshots of the range-based tracking system are shown in Figure 13 for example.

5.2. Results and Discussions

In this section, we present the experiment results of many cases as well as some simulation results which are relevant. Though there are many possible combinations of deployment and comparisons, we have presented most important ones among them in our opinion.

5.2.1. Comparison of range-based algorithms.

In this experiment, three range-based algorithms, C-MMSE, M-MMSE, and W-MMSE have been compared on our test-bed. The person with the target Tmote has changed among 30 different positions in a static manner; that is, at each position, the person stayed for a long time (about 5 min), and when changing the target's position, the raw data during the transition time has been discarded for estimation. All the 30 positions have been taken in the corridor. Accordingly the estimation area of the algorithms has been bounded inside the corridor area.

Figure 14 shows the cumulative distribution function (CDF) of the estimation errors of those 30 positions. The estimation error is defined as the absolute distance which is the difference between the estimated target's location and the actual target's location. In general, W-MMSE outperforms all the algorithms and C-MMSE offers the

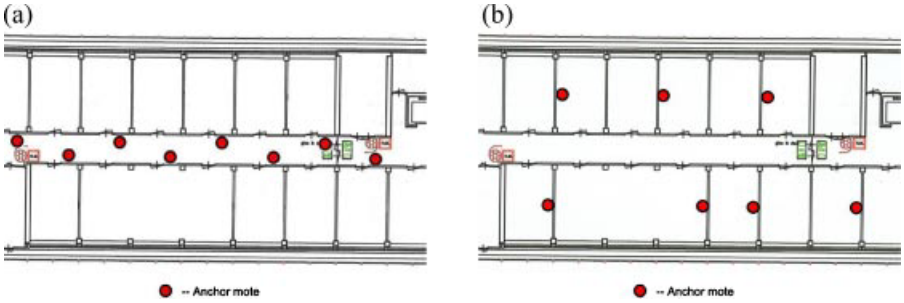

Figure 12. Floor layout and anchor deployment. (a) Anchor deployment for range-based system. (b) Anchor deployment for range-free system.

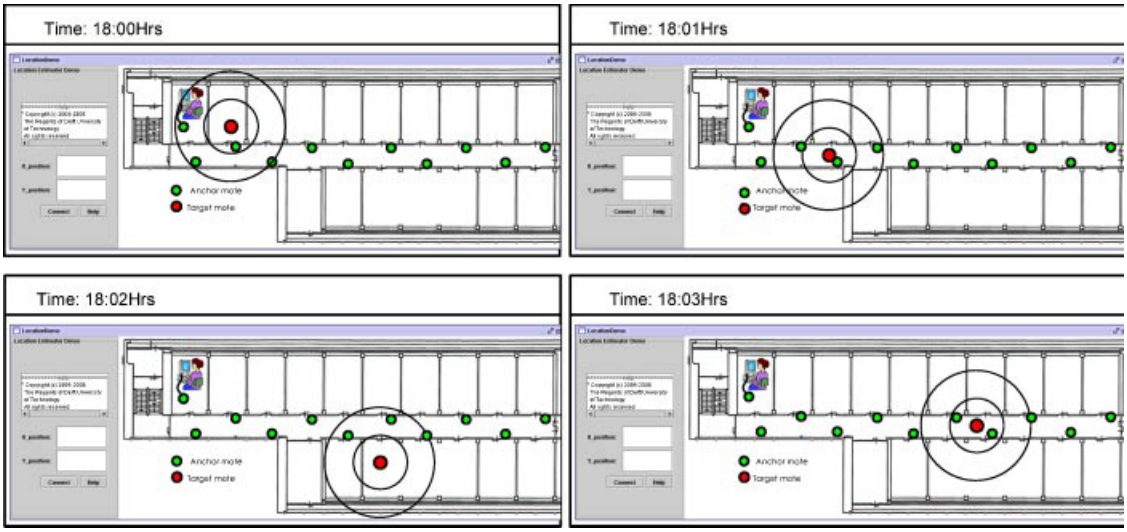

Figure 13. Real-time tracking Java GUI.

lowest performance. For W-MMSE, 25% of the estimated positions are within an absolute error distance of 0.6 m, and 75% estimations within the error of 1.7 m. The results show that W-MMSE gives a better accuracy.

5.2.2. Evaluation and usage of the RSSI generator.

The RSSI generator has been evaluated by comparing the estimation results by using the field RSSI measurement (as given in the previous section) and those using the simulated RSSI values by the generator under the three models. The anchor deployment for this evaluation follows Figure 12(a), considering the RSSI values for the generator construction have been collected under the LOS condition. With the same reason the tested target positions are all in the corridor. For each position estimation different number of generated RSSI values has been used and compared.

The evaluation results of the real model based generator (R-G) and statistical model based generator (S-G) under three different range-based algorithms are shown in Figures 15,16 and 17. In general, the results by using S-G data are closer to that of the real RSSI measurement from the test-bed, comparing to the results by using R-G data. The reason is, R-G generates RSSI values according to the empirical pmf obtained from the field measurement, which cannot exclusively include all the possible RSSI values regarding different transceiver pair placement, thus it loses completeness. Whereas S-G employs the statistical distribution, which not only is a best fit for the measurement, but also adds the RSSI values that has not been observed from the limited measurement samples, but are expected to observe if changing the transceiver pairs placement. In this way, the limitation of the RSSI measurement is alleviated to some extent.

Another observation is that, while decreasing the number of the generated RSSI values for position estimation, the

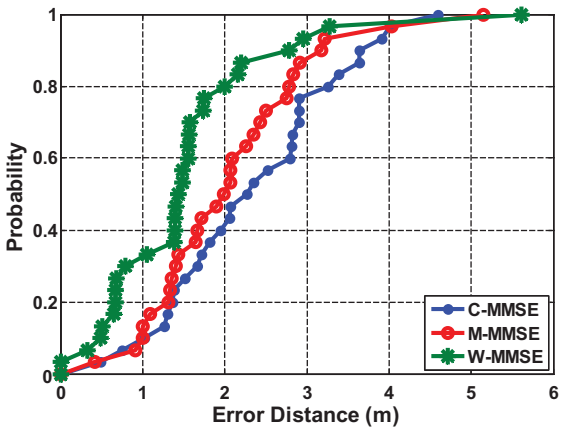

Figure 14. Range-based algorithms comparison.

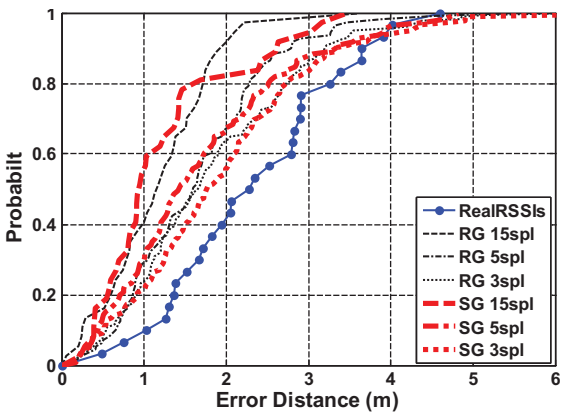

Figure 15. RSSI generator evaluation with C-MMSE.

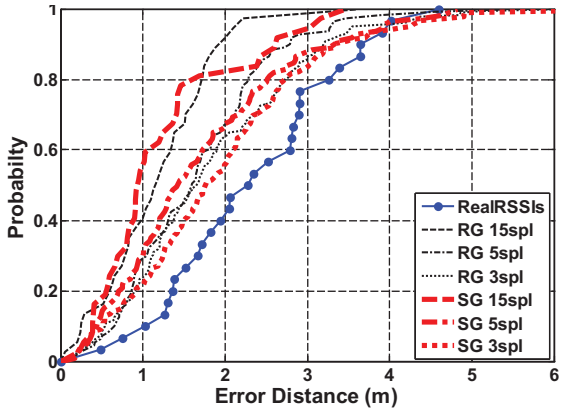

Figure 16. RSSI generator evaluation with M-MMSE.

results have higher estimation error. However, they are closer to the results based on the RSSI field measurement. This reflects that the generators give optimal RSSI samples than the real measurements in terms of giving more accurate position estimation. One reason is that, the RSSI samples for the generators have been collected while placing the sensors in the middle of the corridor, thus the RSSI values have much less variation than those collected when the transmitter and the receiver are randomly placed in any part of the corridor, for example, close to the wall or by the door of the office room. Another reason is that, the generators have been constructed to emphasize the statistical aspect of the RSSI measurement. As a result, by averaging more samples, the dynamics of RSSI at certain distance can be further minimized, which results in less estimation error. Besides, when comparing the results by using different MMSE algorithms, the W-MMSE gives the most consistent results with regard to different generator models and different number of samples. In other words, it can best alleviate the impact of the dynamics of the RSSI for position estimation.

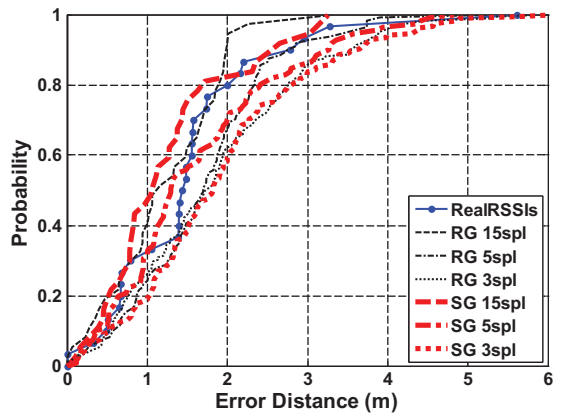

Figure 17. RSSI generator evaluation with W-MMSE.

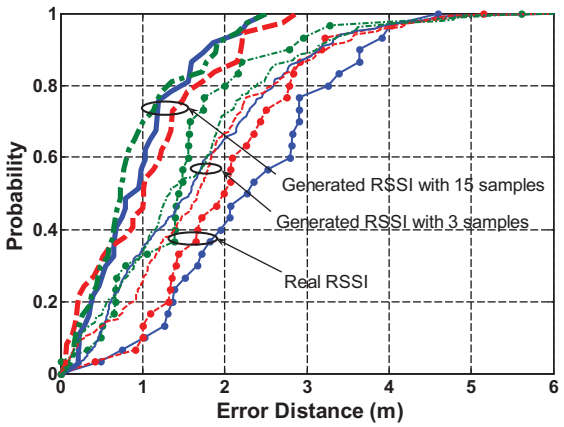

Figure 18. RSSI generator evaluation with MMSE algorithms. (Solid: C-MSSE. M-MMSE, Dash dot: W-MMSE.)

The position estimation results by using the generator with the simplified model are shown in Figures 18 and 19. For this estimation, the confidence level used has been fixed at 95%. Different β_E and sample values have been compared under different range-based algorithms. First we set $\beta_E = 1$, which is the actual degree of variation from the measurement used to generate RSSI values. As shown in Figure 18, less number of samples has been taken for position estimation; the result is closer to that evaluated using the RSSI field measurement. For the same reasoning as explained previously, fewer samples make the generated RSSI values more variable as in the field measurements. Increasing β_E to 120%, 140%, and 160% to extend the upper and lower boundary of the uniform distribution, the estimation results do not have much difference under different β_E as shown in Figure 19. The reason is that, when using the generated RSSI values for position estimation, we have taken the average of the generated RSSI values with respect to number of samples, and used this average in the algorithms. In this way, the averaging process counteracts the randomness added on each generated RSSI value by extending its range with the uniformly distributed random value.

From the generator evaluation experiments, we see all the generators can correctly reflect the relative performance amongst the different algorithms as in the real world. W-MMSE gives the better estimation results than C-MMSE and M-MMSE. Among three generators, we would like to say the statistical distribution based model can best reflect the results from the RSSI field measurement.

5.2.3. Wall effects to range-based system.

To extend the target's activity area from the corridor to the office rooms, we have added a wall model in the range-based algorithms. Because all the anchor Tmotes have been deployed in the corridor, when the person enters the office room the attenuation caused by the walls needs to be taken into account in the estimation. A threshold has been defined to distinguish if the target Tmote is in the corridor or in the office rooms. Because the horizontal distance between two closest neighbor anchors is 4 m, the biggest Euclidean distance between the target Tmote and the nearest anchor

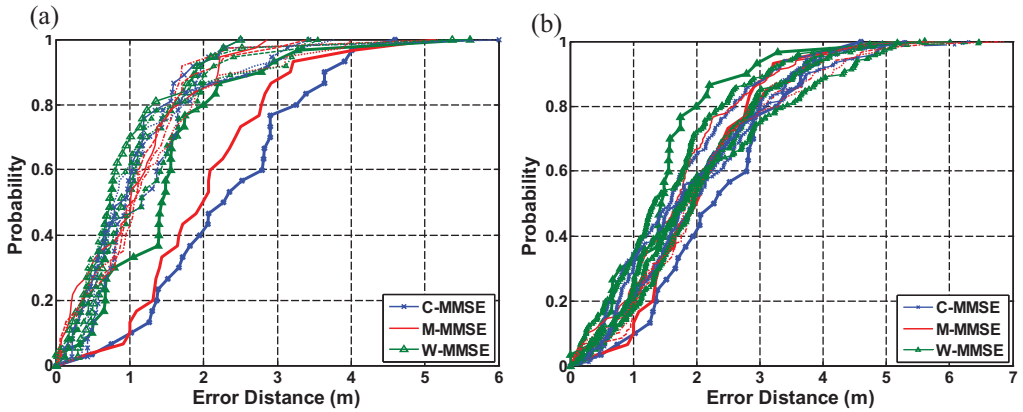

Figure 19. RSSI generator evaluation with different boundaries (Blue cross: C-MMSE, Red: M-MMSE, Green triangle: W-MMSE). (Thick solid: Real RSSI, Thin solid: $\beta_E = 1$, Dash dot: $\beta_E = 1.2$, Dash: $\beta_E = 1.4$, Dot: $\beta_E = 1.6$) (a) 15 Samples per estimation. (b) 3 samples per estimation.

Tmote is 2.5 m as illustrated in Figure 20. According to the calibration measurement, we take the smallest RSSI value amongst four different antenna directions at 3 m as the threshold. That is, if the corresponding distance of the largest measured RSSI is longer than 3 m, we consider the target to be in one of the office rooms. According to our measurement, for single wall, 3 dBm attenuation is accounted. Typically, if the target is estimated to be inside the office room, 6 dBm is added to the RSSI value to compensate the wall effect. This is due to the fact that on an average two walls are present including the compartment wall between the target and the anchor. It has been found by many experiments that with 6 dBm attenuation the target position is estimated with lesser error.

We tracked the person in real-time using W-MMSE with the wall effect adjustment. The person has moved from one position to another in a low speed, and recorded the position at definite instants. Figure 21 shows the estimation results obtained when the person was in the corridor and when inside the office rooms. Totally, 36 experimental positions have been recorded in the corridor experiment. Considering the estimation results for all the 36 positions, 50% of the estimations provide an accuracy of about 2 m and 25% of them about 1.5 m. For the cases of the person staying in the office room, 16 experimental positions have been recorded. Twenty five per cent of them have an accuracy of about 3.3 m; and 50% of them were found to be within about 3.8 m. This error is less than the size of the office room. The individual position estimation is able to point out, in most cases, the exact room the person is currently staying. There are some cases where it may be difficult to say which room the person is in, at a moment, for example, if the person is standing in between two rooms or standing in between two rooms in the middle of the corridor. The conclusion in such cases is hard to arrive at; however, continuous monitoring of the position will result in a better understanding of the context, which in turn will be used to conclude the position. This aspect is out of the scope of this paper since it involves a feedback loop between 'context' generator and the positioning systems. We note here that, the possibility of the cases discussed above is very few compared to the persons being inside the rooms.

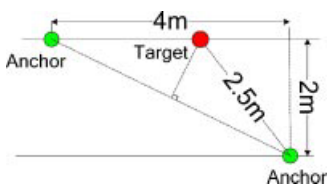

Figure 20. Biggest Euclidian distance estimation.

5.2.4. Comparison of different center of gravity schemes for range-free algorithm.

As discussed previously in the range-free algorithm, the estimated location of the target is the center of gravity of the overlapped area, thus the accuracy is influenced by the centering schemes. In the experiment, all the target positions have been taken inside the rooms. Three schemes

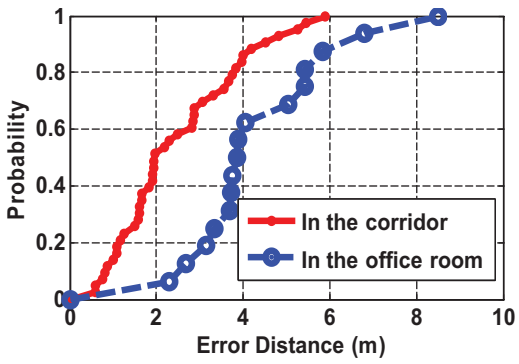

Figure 21. Real-time experiment performance by using W-MMSE.

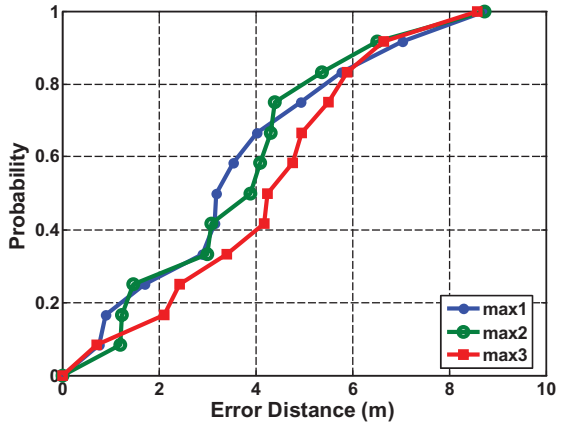

Figure 22. Comparison with different gravity centering scheme of the range-free algorithm.

have been compared, as shown in Figure 22. The 'max-3' scheme gives the worst performance since it takes into accounts too many grids with lower values. Those low value grids overshadow the contribution from high value grids, which carry the more reliable information, and thus degrade the estimation result. The 'max-1' and the 'max-2' schemes achieve similar accuracy. In some cases, 'max-2' outperforms 'max-1' indicating that the proper amount of adjustment from the 'not so reliable' area can help to balance the bias from the 'highly reliable' area. This bias comes from the unreliable rings due to the unstable RSSI values.

5.2.5. Comparison of weighing schemes for range-free algorithm.

For this comparison, we have used the 'max-2' center of gravity scheme, but changed the power index of the weighing parameter. According to the results depicted in Figure 23, an index value of 0.5 gives the best performance, and an index of 2.0 degrades the performance. The difference in accuracy is quite obvious when the error distance is large. In the best case, the mean error is 3.9 m. the power index in the weighing scheme can be related to the inverse exponential index in the propagation model, and it can be deducted as:

$$[\mathrm{RSSI}]_{dB} = -10\beta \log\left(\frac{A}{d}\right) \Rightarrow d = \left(\frac{A}{10^{\frac{\mathrm{rssi}}{10}}}\right)^{\frac{1}{\beta}} \quad (6)$$

$$d \propto \left(\frac{1}{10^{\frac{\mathrm{rssi}}{10}}}\right)^{\frac{1}{\beta}} \Rightarrow w_{TI} = \left(\frac{1}{10^{\frac{\mathrm{RSSI}_{TI}}{10}}}\right)^{\frac{1}{\beta}} \quad (7)$$

When we compare the simplified approximated expression as in (5), n reflects $1/\beta$ in this sense. As we know from earlier studies on the propagation model, in the indoor environment, β takes values from 1.6 to 1.8 [34] in line-of-sight cases, and ranges from 4 to 6 when obstructed. This may shed some light on the reason that n with value 0.5 gives the best performance.

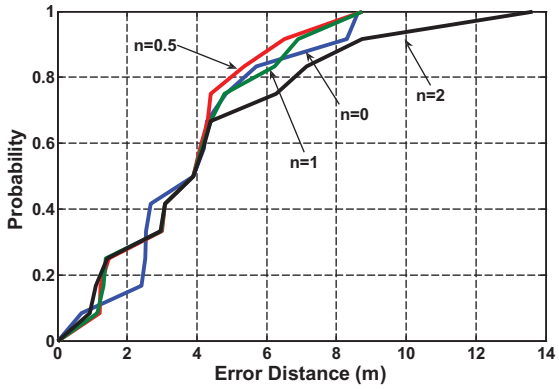

Figure 23. Comparison with different power index of the range-free algorithm.

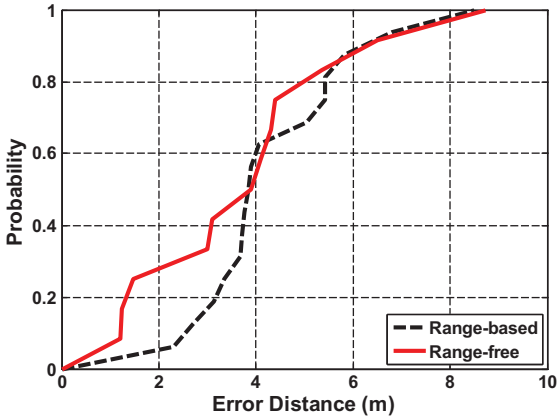

Figure 24. Comparison of range-based and range-free systems.

5.2.6. Comparison of range-based and range-free systems.

We have compared our range-free system with our range-based system using W-MMSE algorithm. The comparison of the in-room estimation is plotted in Figure 24. The result shows promising enhancement in the accuracy for range-free system. The improvement in the small error distance case is noticeable. We note that the two systems taken here for comparison were having different deployment patterns (see Figure 12). However, this is a fair comparison since the deployment pattern selected for each system provides the best possible accuracy for that system.

6. CONCLUSION

In this work, we have presented design, implementation and evaluation of our proposed indoor positioning system, which is considered as an important auxiliary system for providing location information as the input of various context-aware applications. In the course of system design, we have tried to leverage the trade-off between simplicity and accuracy, and also taken into account the real-time requirement from many context-aware applications.

Based on the extensive study on the current indoor positioning systems, we have chosen to the RSSI-based positioning techniques by deploying simple wireless sensors (Tmote Sky). We have developed and implemented both range-based algorithm and range-free algorithm, which are considered as the two main approaches of the RSSI-based techniques, in our test-bed. Comparatively, the range-free algorithm improves the scalability in that it alleviates the laborious off-line work of database creation and RSSI map measurement while maintaining the accuracy. However, the range-based algorithm is less power consuming because instead of all the anchors and the target sending out beacon packets periodically, only the target needs to do that, which is greatly beneficial for the power limited sensors. The field test shows the satisfying results. In 80% cases estimations in the corridor was within the distance error of 2 m by using the range-based W-MMSE algorithm. The room, in which the person stays can be estimated correctly in most of the cases, with an error of one neighboring room in a few cases, and with an error of two neighboring rooms very rarely by both range-based and range-free algorithms.

In addition, the RSSI characteristics of the sensor platform in use have been explored. Three different RSSI generator models have been proposed and evaluated. It shows that, with the proper parameter settings, the RSSI generator is able to simulate RSSI values, which is comparable to the field measurements, and can be used to evaluate different algorithms by avoiding the repetitive experiment setup and data collection works.

From the design and implementation experience, we envisage that a WSN-based positioning system are applicable to—and will be very useful—to monitor the moving targets (e.g., people, mobile devices), when the movement is within people walking speeds. In the ambit of the projects such as 'MAGNET Beyond' [35] and 'Future Home Network' [5] emphasis is on many services that take the location of the person as an important parameter. The critical advantage is that the sensors that are usually deployed can also be used for positioning purpose without additional cost.

As our current test-bed is still relatively a small-scale experiment, within a single floor of an office building, we intend to extend the test-bed to several floors, thus three-dimensional location estimation becomes feasible. Another task which is worthy of exploration is to implant our person tracking system into the location-aware applications to gain more insights on its practical applicability. This is being tested currently on the WPN implementation test-bed.

ACKNOWLEDGEMENTS

The authors thank IST MAGNET Beyond, Dutch national IOP Future Home Network and IOP SiGi Spot projects for partially funding this work. MAGNET Beyond is a continuation of the MAGNET project (www.ist-magnet.org). MAGNET Beyond is a worldwide R&D project within Mobile and Wireless Systems and Platforms Beyond 3G. MAGNET Beyond will introduce new technologies, systems, and applications that are at the same time user-centric and secure. MAGNET Beyond will develop user-centric business model concepts for secure Personal Networks in multi-network, multi-device, and multi-user environments. MAGNET Beyond has 32 partners from 15 countries, among these highly influential Industrial Partners, Universities, Research Centers, and SMEs.

REFERENCES

1. Niebert N, Schieder A, Abramowicz H, Prehofer C, Karl H. Ambient networks: an architecture for communication networks beyond 3G. *IEEE Wireless Communications* 2004; 14–22.
2. Ducatel K, *et al*., 'Scenarios for Ambient Intelligence in 2010', IST Advisory Group (ISTAG), European Commission, Brussels. www.cordis.lu/ist/istag.htm 2001.
3. Aarts E, Marzano S (eds). The New Everyday—Views on Ambient Intelligence. Philips Design: Rotterdam, the Netherlands, 2003.
4. Niemegeers IGMM, Heemstra de Groot SM. Research issues in ad-hoc distributed personal networking. *Wireless Personal Communications* 2003; **26**(2–3): 149–167.
5. Dutch IOP GenGom, Future Home Network project, 'The Project Plan'. 2005.
6. Lammertsma PF. 'Satellite Navigation: GPS & Galileo', by Institute of Information and Computing Sciences, Utrecht University, February. 2005.
7. Bahl P, Padmanabhan VN. RADAR: an in-building rf-based user location and tracking system. In *Proceedings of IEEE INFOCOM2000* Tel-Aviv, Israel March, 2000.
8. Lorincz K, Welsh M. Motetrack: a robust, decentralized approach to rf-based location tracking. *Springer Personal and Ubiquitous Computing* 2006; **11**(6): 489–503.
9. Tang Z, Hile H, Bajracharya S, Jurdak R. PetTracker—pet tracking system using motes. In *Proceedings of the Seventh International Conference on Ubiquitous Computing* (*UbiComp'05*) Tokyo, Japan, 2005.
10. Lau E-E-L, Lee B-G, Lee S-C, Chung W-Y. Enhanced RSSI-based high accuracy real-time user location tracking system for indoor and outdoor environments. *International Journal on Smart Sensing and Intelligent systems* 2008; **1**(2): 534–548.
11. Tmote Sky: www.moteiv.com
12. Hightower J, Boriello G. Location Systems for ubiquitous computing. *IEEE Computer* 2001; **34**(8): 57–66.
13. Mutukrishnan K, Lijding M, Havinga P. Towards smart surroundings: enabling techniques and technologies for localization. In *Proceedings of Location- and Context-*

Awareness: First International Workshop (LoCA 2005), Oberpfaffenhofen Germany, 2005.
14. Savvides A, Han C, Srivastava M. Dynamic fine-grained localization in ad-hoc networks of sensors. In *Proceedings of ACM MobiCom'01, Rome* Italy, July, 2001.
15. Yu K, Oppermann I. Performance of UWB position estimation based on time-of-arrival measurements. In *Proceedings of IEEE Confrerence on Ultrawideband System and Technology* (*UWBST*) Kyoto, Japan, 2004.
16. Deng P, Fan PZ. An AOA assisted TOA positioning system. In *Proceedings of IEEE International Conference on Communication Technology* (*WCC–ICCT 2000*). Beijing, China, 2000.
17. Gezici S, Tian Z, Giannakis G, Kobayashi H, Molisch A, Poor HV, Sahinoglu Z. Localization via ultra-wideband radios. *IEEE Signal Processing Magazine* 2005; **22**(4): 70–84.
18. Jin G, Lu X, Park M. An indoor localization mechanism using active RFID tag. In *Proceedings of IEEE International Conference on Sensor Networks, Ubiquitous, and Trustworthy Computing* 2006.
19. Mao G, Fidan B, Anderson BDO. Wireless Sensor Network Localization Techniques. *Computer Networks* 2007; **51**(10): 2529–2553.
20. Zhang M, Zhang S, Cao J, Mei H. A novel indoor localization method based on received signal strength using discrete fourier transform. In *Proceedings of the First International Conference on Communications and Networking in China* (*ChinaCom'06*) 2006.
21. Ohta Y, Sugano M, Murata M. Autonomous Localization Method in Wireless Sensor Networks. In *Proceedings of Third IEEE International Conference on Pervasive Computing and Communications Workshops 2005* (*PerCom 2005 Workshops*) Kauai Island, USA, 2005.
22. Reichenbach F, Timmermann D. Indoor localization with low complexity in wireless sensor networks. In *Proceedings of IEEE International Conference on Industrial Informatics* August, 2006.
23. Sheu J-P, Chen P-C, Hsu C-S. A distributed localization scheme for wireless sensor networks with improved grid-scan and vector-based refinement. *IEEE Transactions on Mobile Computing* 2008; **7**(9): 1110–1123.
24. Liu C, Wu K, He T. Sensor localization with ring overlapping based on comparison of received signal strength indicator. In *Proceedings of IEEE International Conference on Mobile Ad-hoc and Sensor Systems* Florida, USA, 2004.
25. He T, Huang C, Blum BM, Stankovic JA, Abdelzaher T. Range-free localization schemes for large scale sensor networks. In *Proceedings of the ninth annual international conference on Mobile computing and networking* (*MobiCom 2003*) San Diego, USA, 2003.
26. Niculescu D, Nath B. Ad hoc positioning system (APS). *IEEE GLOBECOM* San Antonio, Texas, USA, November, 2001.
27. Shang Y, Ruml W, Zhang Y, Fromherz M. Localization from connectivity in sensor networks. *IEEE Transactions on Parallel and Distributed Systems* 2004; **15**(11): 961–974.
28. Chipcon: www.chipcon.com
29. TinyOS: http://www.tinyos.net
30. NesC: nescc.sourceforge.net
31. Polastre J, Szewczyk R, Culler D. 'Telos: enabling ultra-low power wireless research'. In *Proceedings of the Fourth International Conference on Information Processing in Sensor Networks* (*IPSN/SPOTS'05*) Los Angeles, 2005.
32. Tmote Sky Datasheet. www.moteiv.com/products/docs/tmote-sky-datasheet.pdf
33. An X, Wang J, Prasad RV, Niemegeers IGMM. OPT–Online Person Tracking System for Context-awareness in Wireless Personal Network. *ACM/ SIGMOBILE RealMan'06* May, 2006.
34. Rappaport TS. Wireless Communications, Principles & Practice. Upper Saddle River, NJ, Prentice Hall: 1996.
35. IST project, My Personal Adaptive Global NETwork. www.ist-magnet.org

AUTHORS' BIOGRAPHIES

Jing Wang received her B.Sc. degree in Electrical Engineering from Beijing University of Aeronautics and Astronautics, China, in 2003. In 2005, she received her M.Sc. degree on Telecommunications from Delft University of Technology, the Netherlands. She is now a Ph.D. student in Wireless and Mobile Networks (WMC) group in Delft University of Technology, and working on Dutch IOP GenCom 'Future Home Networks' project. Her present research interests are wireless mesh networks, high data rate wireless personal networks, wireless sensor networks, cognitive networking, and self-organization systems.

R. Venkatesha Prasad received his Bachelor's degree in Electronics and Communication Engineering and M.Tech degree in Industrial Electronics from University of Mysore, India in 1991 and 1994. He received a Ph.D. degree in 2003 from Indian Institute of Science, Bangalore India. During 1996, he was working as a consultant and project associate for ERNET Lab of ECE at Indian Institute

of Science. While pursuing the Ph.D. degree from 1999 to 2003 he was also working as a consultant for CEDT, IISc, Bangalore for VoIP application developments as part of Nortel Networks sponsored project. In 2003, he was heading a team of engineers at the Esqube Communication Solutions Pvt. Ltd. Bangalore for the development of various real-time networking applications. Currently, he is a part time consultant to Esqube. From 2005 till date he is a senior researcher at Wireless and Mobile Communications group, Delft University of Technology working on the EU funded projects MAGNET/MAGNET Beyond and PNP-2008 and guiding graduate students. He is an active member of TCCN, IEEE SCC41, and reviewer of many Transactions and Journals. He is the recipient of outstanding contributor award for his work on IEEE P1900.2 standard. He is on the TPC of many conferences including ICC, GlobeCom, ACM MM, ACM SIGCHI, etc. He is the TPC co-chair of CogNet workshop in 2007, 2008 and 2009 and E2Nets (2010) at IEEE ICC. He is also running PerNets workshop from 2006 with IEEE CCNC. He is the tutorial co-chair of CCNC 2009 and demo chair of IEEE CCNC 2010.

Xueli An received her Bachelors degree in the department of Communications and Electronic Engineering from Harbin Institute of Technology, P.R. China, in July 2003. She received her Masters degree from the faculty of Electrical Engineering, Mathematics, and Computer Science (EEMCS) from Delft University of Technology (TU Delft), the Netherlands, in August 2005. Since September 2005, she is a Ph.D. candidate at the Wireless and Mobile Communications (WMC) Group in TU Delft. Her present research interests involve higher layer protocols design in 60 GHz based wireless *ad hoc* networks, performance analysis of *ad hoc* and sensor networks.

Ignas G. M. M. Niemegeers received his a degree in Electrical Engineering from the University of Gent, Belgium, in 1970. In 1972, he received an M.Sc.E. degree in Computer Engineering and in 1978 a Ph.D. degree from Purdue University in West Lafayette, Indiana, U.S.A. From 1978 to 1981 he was a designer of packet switching networks at Bell Telephone Mfg. Cy, Antwerp, Belgium. From 1981 to 2002 he was a professor at the Computer Science and the Electrical Engineering Faculties of the University of Twente, Enschede, the Netherlands. From 1995 to 2001 he was scientific director of the Centre for Telematics and Information Technology (CTIT) of the University of Twente, a multi-disciplinary research institute on ICT and applications. Since May 2002 he holds the chair Wireless and Mobile Networks at Delft University of Technology, where he is heading the Centre for Wireless and Personal Communication (CWPC). He is an active member of the Wireless World Research Forum (WWRF) and IFIP TC-6 Working Group on Personal Wireless Communication. He was involved in many European research projects, in particular ACTS TOBASCO, ACTS PRISMA, ACTS HARMONICS, RACE MONET, RACE INSIGNIA and RACE MAGIC. His present research interests are wireless and mobile networks, *ad hoc* networks, personal area networks and personal networks, mobile IP and ubiquitous computing and communication.